Analysis of γ'-Fe_4N and soft mode phase transitions: A First Principles Study

Adesh Rohan Mishra,* Gülsüm Efsun Tekneci,† and Vipin Balan‡

(Dated: December 6, 2020)

Abstract: Spin-polarized structural properties of γ'-Fe_4N (Pm-3m) and a lower symmetry structure (P2/m) corresponding to the M-Phonon instability at 10GPa pressure have been studied using the first-principles calculations based on Density Functional Theory. It was observed that at 10GPa and 30GPa, there are presence of negative (imaginary) in the phonon spectrum of γ'-Fe_4N corresponding to the M-point and X-point respectively. It was found that at 10GPa, there is a phase transition from Pm-3m (higher symmetry) to P2/m (lower symmetry). Similarly, there is another phase transition corresponding to the X-instability and a lower symmetry structure has been predicted for that.

Keywords: γ'-Fe_4N, M-instability, X-instability, soft modes.

I. INTRODUCTION

Magnetic, elastic and electronic properties of γ'-Fe_4N alloy have been widely investigated, both theoretically and experimentally for magnetic resonance imaging, high-density magnetic recording applications and as a precursor in NH_3 production. Due to calculated mechanical properties, it is found to be ductile and damage-tolerant. Also all iron nitrides are good metallic conductors.

With a Pm-3m space group γ'-Fe_4N has a face centered cubic structure with a N atom in the body center. Although γ Fe which has fcc structure has no magnetic properties, insertion of N in its body center, it becomes γ'-Fe_4N which is ferromagnetic. It has two inequivalent iron sites with one occupying corners(Fe) and other in the face center positions(Fe) of the system. The octahedral interstitial occupied by N leads to shortening of Fe-N than the distance between Fe-N .

This paper is an attempt to recreate the work done by Tai-min Cheng et al. work on spontaneous magnetization-induced phonons stability in γ'-Fe_4N crystalline alloys and high-pressure new phase which studied the stability of lattice dynamics and magnetization of of ordered γ'-Fe_4N crystalline alloy at high pressure using first principle calculations carried out with VASP code. Therefore geometry of γ'-Fe_4N alloy was optimized and M-instability under 10 GPa pressure was investigated , along with a structure prediction for the X-instability was done using Quantum ESPRESSO code for comparison with the work done by VASP code.

II. COMPUTATIONAL METHOD

The calculations are performed based on the Density Functional Theory (DFT) using the Generalized Gradient Approximation (GGA) method in the scheme of Perdew- Burke-Ernzerhof (PBE). Plane-wave pseudopotential method as implemented in the Quantum ESPRESSO software package have been used. The initial part of the calculations which are computationally less intensive have been carried out using a mesh of 10x10x10 as well as a 6x6x6 mesh in order to model the first Brillouin zone, but the later parts of the calculations which were computationally more intensive were carried out using only a mesh of 6x6x6. Similarly, for the convergence test results, a kinetic energy cutoff of 101 Ry was used to brief the plane wave expansion of the Kohn-Sham wave functions for computationally more intensive tasks and for the computationally less intensive tasks, cutoff value of 60 Ry was used. All these values that have been used are in complete agreement with the results obtained from the convergence tests and have been mentioned in the respective sections.

In order to determine properties like the equilibrium lattice constants, the total energy of the system for different values of lattice parameters/unit cell volumes has been calculated and then the results are fitted into the Murnaghan equation of state.

III. CONVERGENCE TESTING

For obtaining the reliable values of K-mesh, cutoff for charge density (ecutrho), cutoff for wavefunctions (ecutwfc) as well as the starting magnetization values, independent convergence tests have been carried out and the obtained results have been presented in the appendices section of this report. For the convergence of K-mesh and cutoff for wavefunctions, the effect on the deviation of hydrostatic pressures have been observed. The (ecutrho/ecutwfc) factor was investigated to obtain the value of charge density cutoff to be used. Lastly, the value of the starting magnetization was optimized in order to carry out spin-polarized calculations. The time of computation was also observed in each case. All the observed convergence results have been reported in the appendix section.

* mishra.adeshrohan76@gmail.com
† efsun.tekneci@gmail.com
‡ ksvipinbalan@gmail.com

IV. RESULTS AND DISCUSSION

A. $\gamma' - Fe_4N$:

Having obtained the optimal settings, the DFT calculations were run for the γ'-Fe_4N. After the complete geometry optimization was carried out, it was observed that γ'-Fe_4N has a Pm-3m equilibrium crystal structure. The equilibrium lattice parameter was determined to be 3.7926 Angstroms which is in complete agreement with the value of 3.795 Angstroms as reported by Tai-min Cheng et. al. Figure 2 shows the energy per formula unit fitted into the Murnaghan equation of state, which has been plotted against the unit cell volume (for 101Ry and 10x10x10 setting as well as 60Ry and 6x6x6 settings respectively). Some important properties of the equilibrium structure such as calculated Bulk Modulus (B_0), first derivative of the Bulk Modulus (B_0') as well as the magnetic moment have been given in Table 1. From the equation of state fit, the volume and energies per formula unit for the Pm-3m structure close to 3 different pressures, namely 10GPa, 30GPa as well as 40GPa have been noted in Table 2. The percentage volume change obtained in case of 10GPa and 30GPa are -5.217% and -13.4% respectively, which is in agreement with the provided results.

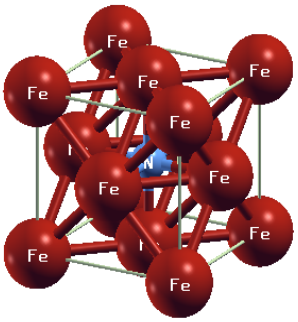

FIG. 1. Equilibrium crystal structure Pm-3m of γ'-FeN

TABLE I. Equilibrium Lattice Constant(a_0), Bulk Modulus (B_0), first derivative of the Bulk Modulus (B_0') and Magnetic moment(μ_B) at equilibrium (using higher precision settings).

a_0(Ang)	B_0(GPa)	B_0'	Magnetic moment(μ_B)
3.7926	172.6	4.32	10.00

B. The M-instability:

As shown in the study by Tai-min Cheng et. al., there is an appearance of the negative (imaginary) frequencies at the M-point (the soft mode) in the phonon spectrum of γ'-Fe_4N at 10GPa, which implies that the crystal loses stability at this pressure value and the crystal symmetry breaks and there is a phase transition to a low-symmetry crystal structure.

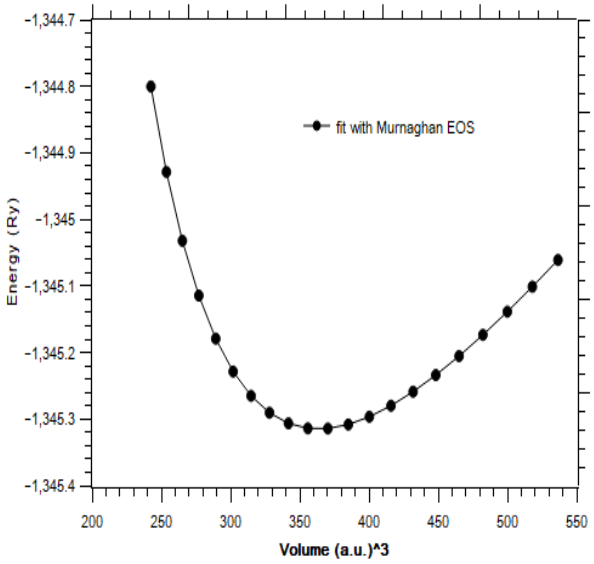

FIG. 2. E(V) curve of γ'-Fe_4N fitted with the Murnaghan Equation of State [spin polarization and high precision settings used(10x10x10 and 101Ry)]

TABLE II. Energies corresponding to different pressure values according to the equation of state. [spin polarization and lower precision settings(6x6x6 and 60Ry) used for comparison with the next section]

Pressure	Volume(au^3)	Energy(Ry)
10GPa	344.6024	-1345.26435
30GPa	314.8503	-1345.22246
40GPa	308.3364	-1345.20619

A distorted supercell (Figure 4) with the distortion corresponding to the M-phonon was constructed and DFT calculations were conducted. After a complete geometry optimization, the structure crystallized into a P2/m crystal structure. The E(V) curve fitted to the non-cubic Murnaghan equation is shown in Figure 5.

The values of volume and energies per formula unit corresponding to the pressures of 10GPa, 30GPa as well as 40GPa have been in the table 4.

On comparing the total energy per formula unit at 10 GPa from the table 2 and table 4, it can be clearly observed that the P2/m – Fe4N is more stable as compared to the Pm-3m – Fe4N at this pressure value. Thus,there will a phase transition from the Pm-3m crystal structure to P2/m crystal structure at a pressure of 10GPa.

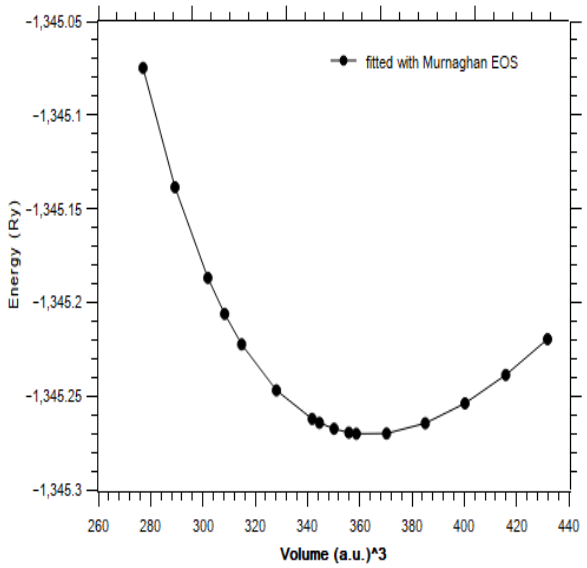

FIG. 3. E(V) curve of γ'-Fe_4N fitted with the Murnaghan Equation of State [spin polarization and low precision settings used(6x6x6 and 60Ry)]

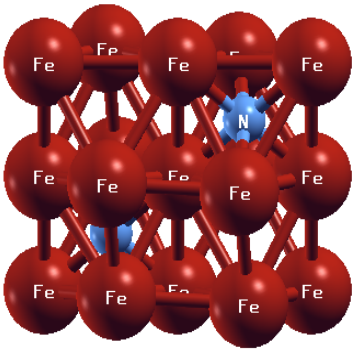

FIG. 4. Supercell of P2/m Fe_4N with distortion corresponding to the M-phonon

C. The X-instability:

Similarly, there is another appearance of of the negative (imaginary) frequencies at the X-point (another soft mode) in the phonon spectrum of γ'-Fe_4N at 30GPa.

In order to obtain the distorted crystal structure associated with the distortion corresponding to the X-phonon was obtained using the ISODISTORT module.

One such distorted crystal structure obtained from the ISODISTORT module with a distortion corresponding to the X-phonon has been visualized as shown in Figure 6 which forms a C2/m crystal structure. Due to a lack of computational time and resources, we were unable to carry out the DFT calculations for this part.

TABLE III. Equilibrium Volume(a_0), Bulk Modulus (B_0), first derivative of the Bulk Modulus (B_0') and Magnetic moment(μ_B) for the P2/m supercell [using lower precision settings(60Ry and 6x6x6)].

$V_0(au^3)$	B_0(GPa)	B_0'	Magnetic moment(μ_B)
728.74	163.8	4.70	17.62

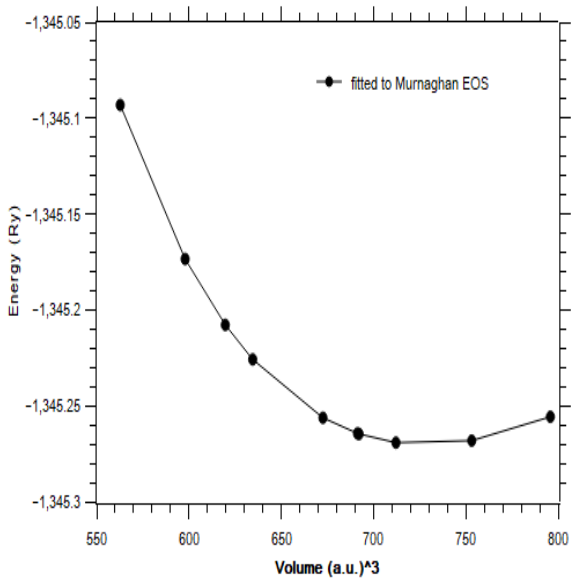

FIG. 5. E(V) curve of P2/m-Fe_4N fitted with the Murnaghan Equation of State [spin polarization and low precision settings used(6x6x6 and 60Ry)]

TABLE IV. Energies corresponding to different pressure values according to the equation of state. [spin polarization and lower precision settings(6x6x6 and 60Ry)] for P2/m structure.

Pressure	Volume(au^3)	Energy(Ry)
10GPa	691.31	-1345.264425
30GPa	634.53	-1345.226155
40GPa	619.71	-1345.20783

V. CONCLUSIONS

In this work, we analyzed different properties of γ'-Fe_4N. The equlibrium lattice parameter for Pm-3m γ'-Fe_4N is 3.7926 Angstroms. The volumes and energies per formula unit were analyzed for the pressure values of 10GPa, 30GPa as well as 40 GPa.

It was also concluded that at 10 GPa, the P2/m structure (lower symmetry) is more stable than the Pm-3m structure. This is in complete agreement with the previously found soft mode at the M-point in the phonon spectrum. A similar soft mode is also seen at 30 GPa that corresponds to the X-Phonon. A possible crystal structure (C2/m) was suggested.

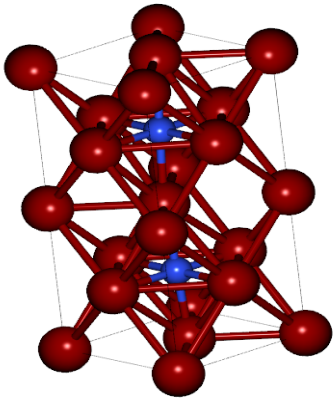

FIG. 6. Supercell of Fe_4N with distortion corresponding to the X-phonon

ACKNOWLEDGMENTS

We want to thank Prof. Dr. Stefaan Cottenier for giving us this wonderful opportunity to enhance our learning through this project and for his constant support throughout each and every step of the project.

[1] P. Giannozzi, S. Baroni, N. Bonini, M. Calandra, R. Car, C. Cavazzoni, D. Ceresoli, G. L. Chiarotti, M. Cococcioni, I. Dabo, *et al.*, Quantum espresso: a modular and open-source software project for quantum simulations of materials, Journal of physics: Condensed matter **21**, 395502 (2009).

[2] H. Jacobs, D. Rechenbach, and U. Zachwieja, Structure determination of γ-fe4n and -fe3n, Journal of Alloys and Compounds **227**, 10 (1995).

[3] T.-m. Cheng, G.-l. Yu, Y. Su, L. Zhu, and L. Li, Spontaneous magnetization-induced phonons stability in γ-fe4n crystalline alloys and high-pressure new phase, Journal of Magnetism and Magnetic Materials **451**, 87 (2018).

[4] X. Bao, R. M. Metzger, and W. D. Doyle, Synthesis of high moment and high coercivity iron nitride particles, Journal of applied physics **73**, 6734 (1993).

[5] Y.-R. Jang, I. Kim, and J. Lee, Electronic structure and magnetic properties of fe4n (0 0 1), Journal of magnetism and magnetic materials **263**, 366 (2003).

[6] A. Nozik, J. Wood Jr, and G. Haacke, High resolution mössbauer spectrum of fe4n, Solid State Communications **7**, 1677 (1969).

[7] C.-H. Cheng, M.-T. Nguyen, T.-S. Leu, I. Chang, M.-L. Liao, S. V. Panin, A. V. Panin, *et al.*, Magnetic and mechanical properties of deformed iron nitride-fe4n, Journal of Applied Mathematics **2015** (2015).

[8] T. Yamaguchi, M. Sakita, M. Nakamura, and T. Kobira, Synthesis and characteristics of fe4n powders and thin films, Journal of magnetism and magnetic materials **215**, 529 (2000).

[9] P. Emmett, S. Hendricks, and S. Brunauer, The dissociation pressure of fe4n, Journal of the American Chemical Society **52**, 1456 (1930).

[10] E. L. P. y. Blancá, J. Desimoni, N. E. Christensen, H. Emmerich, and S. Cottenier, The magnetization of γ-fe4n: theory vs. experiment, physica status solidi (b) **246**, 909 (2009).

[11] H. Stokes, D. Hatch, and B. Campbell, Isodistort, isotropy software suite (2019).

[12] M. I. Aroyo, J. M. Perez-Mato, C. Capillas, E. Kroumova, S. Ivantchev, G. Madariaga, A. Kirov, and H. Wondratschek, Bilbao crystallographic server: I. databases and crystallographic computing programs, Zeitschrift für Kristallographie-Crystalline Materials **221**, 15 (2006).

Appendix: Convergence Tests

Low Precision Settings: (6x6x6)

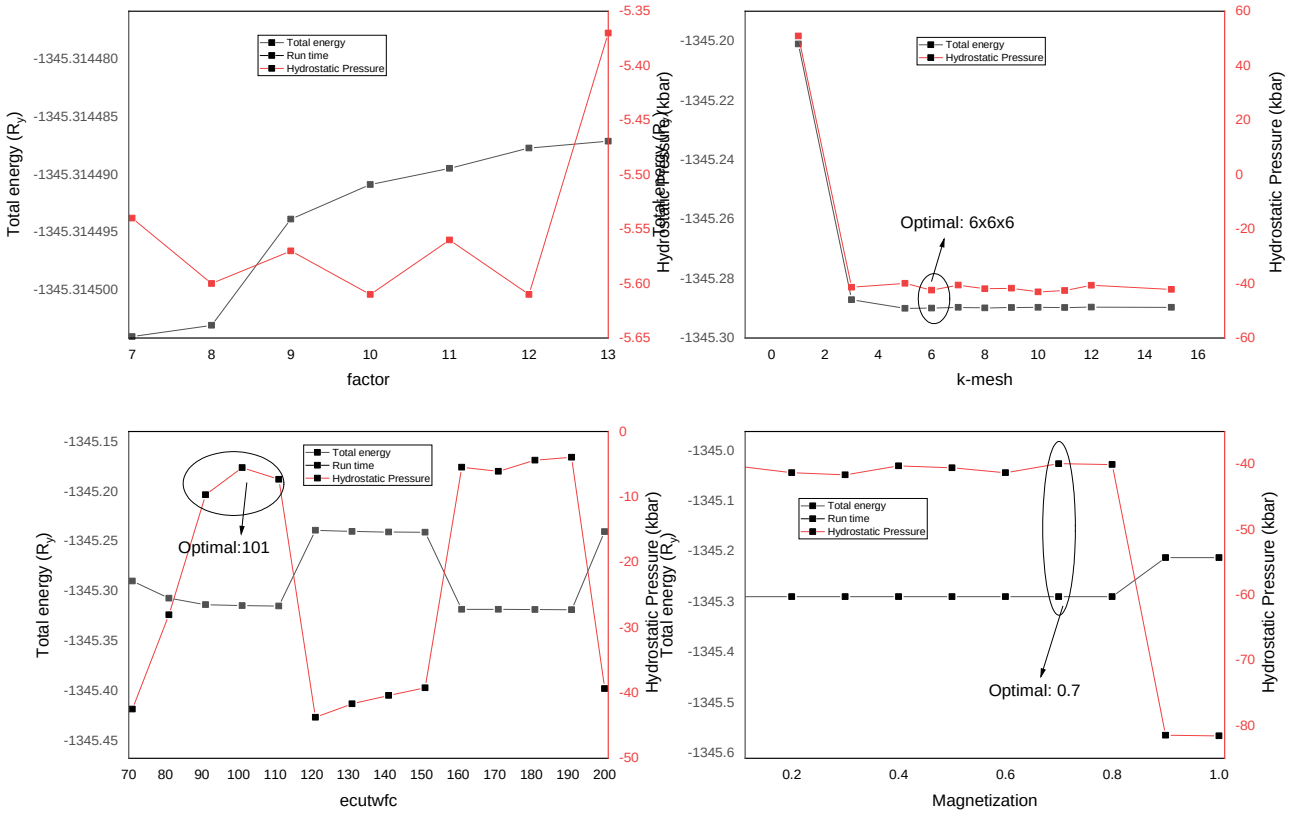

High-precision settings: (10x10x10)

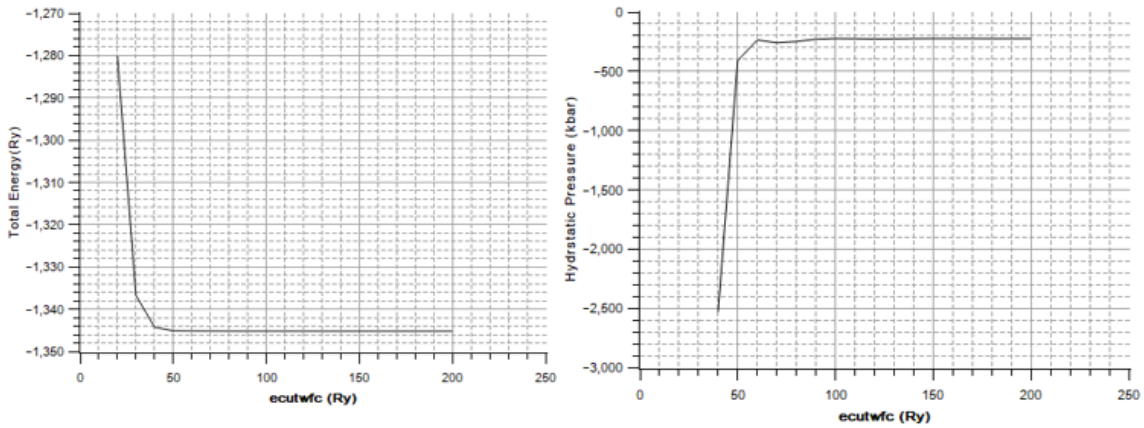

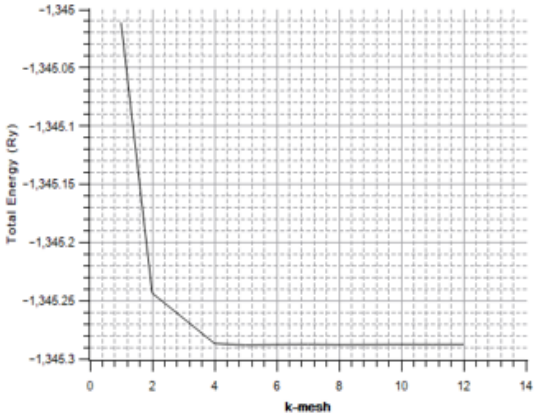
Total Energy (Ry)
-1,345
-1,345.05
-1,345.1
-1,345.15
-1,345.2
-1,345.25
-1,345.3
0
2
4
6
8
10
12
14
k-mesh

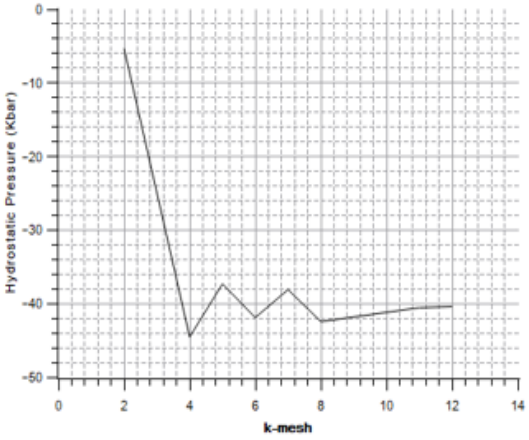
Hydrostatic Pressure (Kbar)
0
-10
-20
-30
-40
-50
0
2
4
6
8
10
12
14
k-mesh

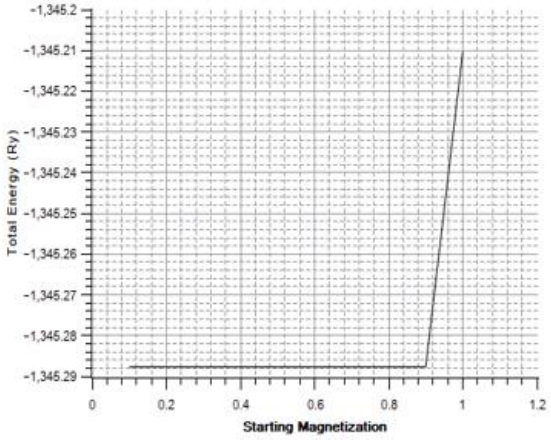
Total Energy (Ry)
-1,345.2
-1,345.21
-1,345.22
-1,345.23
-1,345.24
-1,345.25
-1,345.26
-1,345.27
-1,345.28
-1,345.29
0
0.2
0.4
0.6
0.8
1
1.2
Starting Magnetization

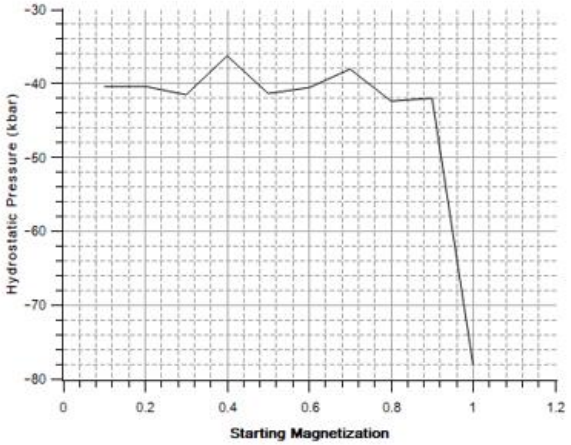
Hydrostatic Pressure (kbar)
-30
-40
-50
-60
-70
-80
0
0.2
0.4
0.6
0.8
1
1.2
Starting Magnetization